Neurobiology of Disease

Rescue of Glaucomatous Neurodegeneration by Differentially Modulating Neuronal Endoplasmic Reticulum Stress Molecules

Liu Yang,[1]* Shaohua Li,[1,4]* Linqing Miao,[1]* Haoliang Huang,[1] Feisi Liang,[1] Xiuyin Teng,[1] Lin Xu,[1,5] Qizhao Wang,[2] Weidong Xiao,[2] William H. Ridder III,[6] Toby A. Ferguson,[7] Dong Feng Chen,[8] Randal J. Kaufman,[9] and Yang Hu[1,3]

[1]Center for Neural Repair and Rehabilitation, Shriners Hospitals Pediatric Research Center, [2]Sol Sherry Thrombosis Research Center, and [3]Department of Anatomy and Cell Biology, School of Medicine, Temple University, Philadelphia, Pennsylvania 19140, [4]Department of Ophthalmology, Union Hospital, Tongji Medical College, Huazhong University of Science and Technology, Wuhan 430022, China, [5]Department of Neurology, Affiliated Hospital of Qingdao University, Qingdao 266000, China, [6]Southern California College of Optometry, Marshall B. Ketchum University, Fullerton, California 92831, [7]Amyotrophic Lateral Sclerosis Innovation Hub, Development Sciences, Biogen Idec, Cambridge, Massachusetts 02142, [8]Department of Ophthalmology, Schepens Eye Research Institute, Massachusetts Eye and Ear, Harvard Medical School, Boston, Massachusetts 02114, and [9]Degenerative Diseases Program, Sanford Burnham Prebys Medical Discovery Institute, La Jolla, California 92037

Axon injury is an early event in neurodegenerative diseases that often leads to retrograde neuronal cell death and progressive permanent loss of vital neuronal functions. The connection of these two obviously sequential degenerative events, however, is elusive. Deciphering the upstream signals that trigger the neurodegeneration cascades in both neuronal soma and axon would be a key step toward developing the effective neuroprotectants that are greatly needed in the clinic. We showed previously that optic nerve injury-induced neuronal endoplasmic reticulum (ER) stress plays an important role in retinal ganglion cell (RGC) death. Using two *in vivo* mouse models of optic neuropathies (traumatic optic nerve injury and glaucoma) and adeno-associated virus–mediated RGC-specific gene targeting, we now show that differential manipulation of unfolded protein response pathways in opposite directions—inhibition of eukaryotic translation initiation factor 2α-C/EBP homologous protein and activation of X-box binding protein 1—promotes both RGC axons and somata survival and preserves visual function. Our results indicate that axon injury-induced neuronal ER stress plays an important role in both axon degeneration and neuron soma death. Neuronal ER stress is therefore a promising therapeutic target for glaucoma and potentially other types of neurodegeneration.

Key words: **axon degeneration; ER stress; glaucoma; neuroprotection; optic nerve; retinal ganglion cell**

Significance Statement

Neuron soma and axon degeneration have distinct molecular mechanisms although they are clearly connected after axon injury. We previously demonstrated that axon injury induces neuronal endoplasmic reticulum (ER) stress and that manipulation of ER stress molecules synergistically promotes neuron cell body survival. Here we investigated the possibility that ER stress also plays a role in axon degeneration and whether ER stress modulation preserves neuronal function in neurodegenerative diseases. Our results suggest that neuronal ER stress is a general mechanism of degeneration for both neuronal cell body and axon, and that therapeutic targeting of ER stress produces significant functional recovery.

Introduction

CNS axonopathy is a common characteristic not only of acute neural injuries, such as stroke, traumatic brain injury and spinal cord injury, but also of chronic neurodegenerative diseases, including Alzheimer's disease (AD), Parkinson's disease (PD), amyotrophic lateral sclerosis (ALS), hereditary spastic

Received Oct. 8, 2015; revised April 25, 2016; accepted April 26, 2016.

Author contributions: L.Y., S.L., L.M., and Y.H. designed research; L.Y., S.L., L.M., H.H., F.L., X.T., L.X., Q.W., W.X., and Y.H. performed research; Q.W., W.X., W.R.I., T.A.F., D.F.C., and R.J.K. contributed unpublished reagents/analytic tools; L.Y., S.L., L.M., H.H., F.L., L.X., W.R.I., R.J.K., and Y.H. analyzed data; L.Y., S.L., L.M., L.X., and Y.H. wrote the paper.

This work was supported by NIH Grants EY023295 and EY024932 (Y.H.) and DK042394, DK088227, and HL052173 (R.J.K.), BrightFocus Foundation Grant G2013046 (Y.H.), Fight for Sight Grant FFS-GIA-13-008 (Y.H.), National Multiple Sclerosis Society Grant RG5021A1 (Y.H.), and postdoctoral fellowships from Shriners Hospitals for Children (L.Y., L.M.). We thank Dr. Steven Nusinowitz for consultation regarding visual evoked potential analysis, Dr. Kevin Park for providing the shRNA vector, and Drs. Michael Selzer, George Smith, Alan Tessler, and Zhigang He for critically reading this manuscript.

paraplegia, multiple sclerosis (MS), and glaucoma (Coleman and Perry, 2002; Raff et al., 2002; Wang et al., 2012; Conforti et al., 2014). Axonopathies result in axon degeneration, which is followed by retrograde neuronal soma atrophy or death. Preventing axon degeneration is, therefore, critical for minimizing the severe consequences of CNS axonopathies and preserving neuronal function. Extensive study of the slow Wallerian degeneration protein (*Wld*^{s}) suggests that signaling pathways that regulate axon degeneration are very different from the apoptosis pathways that regulate neuronal soma degeneration (Whitmore et al., 2005; Calkins and Horner, 2012; Wang et al., 2012; Howell et al., 2013; Conforti et al., 2014). In models of glaucoma, for example, Wld^s delays retinal ganglion cell (RGC) axon degeneration, but has no effect on degeneration of RGC somata (Beirowski et al., 2008), and apoptotic molecule Bax deletion protects RGC somata, but does not prevent axon degeneration (Libby et al., 2005).

The endoplasmic reticulum (ER) is the organelle responsible for synthesis and proper folding of proteins and exerts essential quality control functions. If the ER is overwhelmed by unfolded and misfolded proteins beyond its handling capacity, ER stress develops. The cell then responds to ER stress by activating characteristic signal transduction pathways, which in aggregate are called the unfolded protein response (UPR; Ron and Walter, 2007; Wang and Kaufman, 2012). Three distinct ER-resident proteins sense stress and initiate the UPR pathways: protein kinase RNA-like ER kinase (PERK), inositol-requiring protein-1 (IRE1α), and activating transcription factor-6 (ATF6). PERK phosphorylates and inactivates eukaryotic translation initiation factor 2α (eIF2α) to attenuate general mRNA translation. However, phosphorylated eIF2α (eIF2α-P) induces the expression of a proapoptotic molecule, CCAAT/enhancer-binding protein homologous protein (CHOP), by selectively activating translation of ATF4. IRE1α, a bifunctional enzyme that contains both a Ser/Thr kinase domain and an RNase domain, initiates another UPR pathway. Its RNase activity mediates the splicing of X-box binding protein 1 (XBP-1) mRNA to generate an active (spliced) form of the transcription factor, XBP-1s. XBP-1s targets a set of ER chaperon proteins that may increase ER protein-folding capacity and facilitate degradation of misfolded proteins, which may protect against the detrimental effect of ER stress (Lin et al., 2007). ATF6 is cleaved sequentially by site 1 protease and site 2 protease in Golgi to generate an active transcription factor ATF6 fragment (ATF6f). ATF6 is generally considered cytoprotective, although its downstream effectors have not been completely identified.

ER stress has been linked with many neurodegenerative disorders (Ron and Walter, 2007; Wang and Kaufman, 2012), but appreciation of the clinical importance of neuronal ER stress has just begun (Pennuto et al., 2008; Saxena et al., 2009; Hu et al., 2012; Moreno et al., 2012; Li et al., 2013; Ma et al., 2013b). Previous studies from our laboratory revealed that both acute traumatic injury of the optic nerve (ON) and chronic elevation of intraocular pressure (IOP) induce neuronal ER stress (Hu et al., 2012). We also showed that modulation of two key downstream molecules of ER stress (CHOP and XBP-1) in opposite directions significantly protected the RGC soma in both ON crush model and glaucoma model (Hu et al., 2012). Although neuronal soma and axon degeneration are active autonomous processes with distinct molecular mechanisms, they are clearly connected. In the present study, we demonstrate in two optic neuropathies (traumatic ON injury and glaucoma) that manipulation of the UPR pathways protects both RGC axon and soma and preserves visual function. These results indicate that ER stress is the common upstream signaling mechanism for both neuronal axon and soma degeneration and suggest that targeting ER stress molecules is a promising therapeutic strategy for neuroprotection.

Materials and Methods

Mice. CHOP KO and C57BL/6 WT mice were purchased from The Jackson Laboratory and kept as separated colonies. *eIF2α A/A;fTg* mice were described previously (Back et al., 2009). All mice had a C57BL/6 background, and either sex was randomly used in experiments. For all surgical and treatment comparisons, control and treatment groups were prepared together in single cohorts and the experiment repeated at least twice. All experimental procedures were performed in compliance with animal protocols approved by the Institutional Animal Care and Use Committee at Temple University School of Medicine.

Intravitreal injection of adeno-associated virus, ON crush, and induction of chronic IOP elevation. The procedures have been described previously (Hu et al., 2012; Yang et al., 2014; Miao et al., 2016). The adeno-associated virus (AAV) titers used for this study were in the range of $1.5–2.5 \times 10^{12}$ genome copy (GC)/ml determined by real-time PCR. AAVs were injected intravitreally 2 weeks before ON crush or microbead injection, except in delayed experiments. Four copies of different mouse CHOP RNAi sequences identified from the RNAi Consortium (5′-ATTTCATCTGAGGACAGGACC-3′; 5′-CATAGAACTCTGACTGGAATC-3′; 5′-TTCCGTTTCCTAGTTC TTCCT-3′; 5′-CGATTTCCTGCTTGAGCCGCT-3′) with modified miR-155 stem-loops and GFP were driven by the ubiquitin C promoter in an AAV backbone (Chung et al., 2006), a gift from Dr. K. Park. ON crush was performed 2 weeks following AAV injection ~0.5 mm behind the eyeball. Elevation of IOP was induced unilaterally in anesthetized 8- to 9-week-old mice by anterior chamber injection of fluorescent polystyrene microspheres with a uniform diameter of 10 μm (F8830, Life Technologies). The IOP of both eyes was monitored twice weekly until 8 weeks after microbead injection using the TonoLab tonometer (Colonial Medical Supply) according to product instructions.

Immunostaining and RGC counting. The procedures have been described previously (Hu et al., 2012; Yang et al., 2014; Miao et al., 2016). Antibodies used were mouse or rabbit neuronal class ß-III tubulin (clone Tuj1, 1:200 dilution; Covance), CHOP antibody (MA1-250, 1:100 dilution; Thermo Fisher Scientific), and rat HA (clone 3F10, 1:200 dilution; Roche). For RGC counting, six to nine fields were randomly sampled from peripheral regions of each whole-mount retina preparation to estimate RGC survival. The investigators who counted the cells were blinded to the treatment of the samples. The percentage of RGC survival was calculated as the ratio of surviving RGC numbers in injured eyes compared to contralateral uninjured eyes.

Quantification of surviving axons. Transverse semithin (1 μm) and ultrathin (90 nm) sections of ON were cut on an ultramicrotome (EM UC7; Leica). For the ON crush model, ON sections were collected 2 mm distal to the eye (~1.5 mm distal to the crush site). For the glaucoma model, ON sections were collected 1 mm distal to the eye. The semithin sections were stained with 1% paraphenylenediamine (PPD) in methanol/isopropanol (1:1; Smith, 2002) and were viewed through a 100× lens of a Nikon microscope with a total amplification of 1000×. Sequential images were taken to cover the entire area of the ON without overlap. An area of 21.6×29 μm was cropped from the center of each image, and the surviving axons within the designated area were counted. After counting all the images taken from a single nerve, the mean of the surviving axon number was calculated for each ON. The mean of the surviving axon number in the injured ON was compared to that in the contralateral control ON to yield a percentage of axon survival value. The ultrathin

*L.Y., S.L., and L.M. contributed equally to this work.

T.A.F. is an employee and shareholder of Biogen.

Correspondence should be addressed to Yang Hu, Temple University School of Medicine, 3500 North Broad Street, Philadelphia, PA 19140. E-mail: yanghu@temple.edu.

DOI:10.1523/JNEUROSCI.3709-15.2016

 0270-6474/16/365892-13$15.00/0

sections were imaged by an electron microscope (JEM-1011; JEOL) at 12,000×.

Western blot. Retinas were dissected out from ice-cold PBS-perfused eyes and homogenized (two retinas per sample) and lysed in 100 μl RIPA buffer (50 mM Tris HCl, pH 8.0, 150 mM NaCl, 1% NP-40, 0.5% sodium deoxycholate, 0.1% SDS, 5 mM sodium pyrophosphate, 10 mM sodium fluoride, 1 mM sodium orthovanadate, protease inhibitor cocktail) on ice for 30 min. The homogenates were centrifuged at 12,000 × g for 20 min, and supernatants were subjected to electrophoresis with 10% SDS-PAGE. For ON, the nerve segments (3 mm from eyeball) were dissected and homogenized (two ON per sample) in 80 μl urea/SDS buffer (50 mM Tris HCl, pH 6.8, 8 M urea, 10% SDS, 10 mM sodium EDTA, and 50 mM DTT). Homogenates were then heated at 95°C for 10 min, cooled on ice for 10 min, and heated back to 95°C for another 10 min; finally, the homogenates were centrifuged at 12,000 × g for 20 min, and supernatants were subjected to electrophoresis with 10% SDS-PAGE. After gel transference, nitrocellulose membranes were blocked with Odyssey blocking buffer (LI-COR) for 1 h before incubation with primary antibody at 4°C overnight. After washing three times for 10 min each with PBS, the membranes were incubated with secondary antibodies (IRDye 680RD goat-anti-mouse IgG or IRDye 800CW goat-anti-rabbit IgG; LI-COR) at room temperature for 1 h. The membranes were then washed three times for 10 min each with PBS and scanned using the Odyssey CLx imaging system (LI-COR). The images were analyzed with Image Studio (LI-COR). The primary antibodies used were mouse anti-HA (clone 16B12, 1:2000; Covance), mouse anti-β-Actin (clone AC-15, 1:2000; Sigma), mouse anti-CHOP (MA1-250, 1:200 dilution; Thermo Fisher Scientific), mouse anti-Neurofilament M (NF-M; clone 3H11, 1:1000; Biolegend), and rabbit anti-binding immunoglobulin protein (BiP) (ab32618, 1:200; Abcam).

Visual evoked potential measurements. Mice were implanted with three stainless-steel screws (Amazon, item #B0038QOTZU) in the skull at 2 mm rostral to bregma (reference electrode) and 2.5 mm horizontal to lambda (overlying the primary visual cortex, for the active electrodes). Mice recovered for 1 week before the first visual evoked potential (VEP) measurement. The mice were kept in the dark for 5–10 min before VEP measurement. The pupils were dilated by applying 1% tropicamide sterile ophthalmic solution (Akorn). Mice were placed in the Ganzfeld of the VEP instrument (RETI-port; Roland Consult) in a dark room, and body temperature was maintained at 37°C using a feedback-controlled heating pad (Physitemp Instruments). The VEP was recorded in response to a series of white light flashes of graded intensity from 0.030 cd · s/m^2 to 3.0 cd · s/m^2. The flashes were presented at a frequency of 1 Hz, and 30 flashes were averaged for a response. The first positive peak in the VEP waveform was designated as P1, and the first negative peak as N1. The latency of P1 and N1 were measured 1 week before microbead injection as a baseline and at the end points of 7 weeks postinjection (WPI) for the glaucoma model. The differences between the baseline and end point recordings under different stimulation intensities were calculated and referred to as ΔP1 latency and ΔN1 latency.

Statistics. Data are presented as means ± SEM. We used Student's *t* test for two-group comparisons, one-way ANOVA with Bonferroni's *post hoc* test for multiple comparisons (three or more groups) with one variance, and two-way ANOVA with Bonferroni's *post hoc* test for multiple comparisons (three or more groups) with two variances.

Results

CHOP deletion and XBP-1 activation synergistically promote RGC axon survival after ON acute injuries

To determine whether manipulation of ER stress prevents axon degeneration, we quantified RGC axon survival in semithin transverse sections of ON at 5 d postcrush (dpc). As shown in Figure 1*A*, axon cluster disruption and filamentous astrocyte proliferation were obvious in WT mice, and only 32% of axons survived (Fig. 1*B*). XBP-1s overexpression alone did not promote axon survival, and *CHOP* KO had only a modest, but significant, protection effect. XBP-1s overexpression in combination with *CHOP* KO, however, showed significantly higher axon survival (58%) and relatively intact axon clusters with less astrocyte proliferation. EM studies confirmed axon protection by ER stress manipulation: regular arrangement of axon clusters with homogenous axoplasm and smooth, uniform myelin sheaths in *CHOP* KO mice with XBP-1s overexpression sharply contrasted with vacuolization and dense accumulation of axoplasm and irregular myelin sheaths in WT mice (Fig. 1*C*). As another test of axon protection, we measured the levels of neurofilament medium chain (NF-M), one of the major axonal cytoskeleton components, in ON after crush. NF-M levels were significantly increased in *CHOP* KO mice with XBP-1s overexpression compared to WT mice after ON crush, but not in single treated mice (Fig. 1*D*). We confirmed that AAV-XBP-1s injection increased the retinal level of HA-tagged XBP-1s and its downstream molecule BiP (Fig. 1*E*). Thus, *CHOP* deletion and XBP-1 activation synergistically promote RGC axon survival after ON crush.

Because similar UPR manipulation also promotes RGC soma survival (Hu et al., 2012), the axon protection effect may be secondary to neuroprotection of the RGC cell body and/or due to a local effect directly on the axon. We then studied the effects of ON cut, which completely separates the RGC somata in retina from their axons in the ON and therefore interrupts communication between them. Survival of RGC somata and axons should therefore be independent of each other. Axon survival was lower after ON cut than after crush, but *CHOP* deletion together with XBP-1s overexpression increased axon survival significantly compared to WT control (Fig. 1*F*), suggesting that ER stress manipulation acts, at least in part, by an axonal autonomous neuroprotection effect. We detected similar axon protection in *CHOP* KO mice with XBP-1s overexpression as early as at 3 dpc (Fig. 2*A*,*B*). However, Western blot analysis did not detect significant degradation of NF-M in ON at 3 dpc (Fig. 2*C*), suggesting the low sensitivity of this assay.

ER stress manipulation prevents glaucomatous RGC axon degeneration

Glaucoma causes progressive RGC axon and soma loss and is the most common cause of irreversible blindness (Quigley and Broman, 2006). Since ER stress manipulation is neuroprotective for RGC soma in the mouse glaucoma model (Hu et al., 2012) and protects RGC axons following ON crush, we tested whether it also protected glaucomatous axons. We injected microbeads into the anterior chamber of the left eyes of adult mice to elevate IOP by blocking aqueous outflow (Fig. 3*A*); the right eyes received a sham injection and served as control. Histology of the anterior segment of the eyeball showed accumulation of microbeads at the corner of the anterior chamber (Fig. 3*B*). The IOP of the mouse eyes was measured once before and twice weekly after microbead injection (Fig. 3*C*). We examined axon survival only in mice with sustained high IOP (≥7 mmHg difference between the microbead-injected and contralateral sham-injected eyes). In WT mice, ~71% of RGC axons were present at 8 weeks after microbead injection. XBP-1 activation alone did not increase glaucomatous axon survival, whereas surviving axons were significantly increased in *CHOP* KO mice with or without AAV-XBP-1s (Fig. 3*D*,*E*). The protective effect was not due to differences in IOP levels, because microbead injection elevated IOP similarly in all experimental groups (Fig. 3*C*).

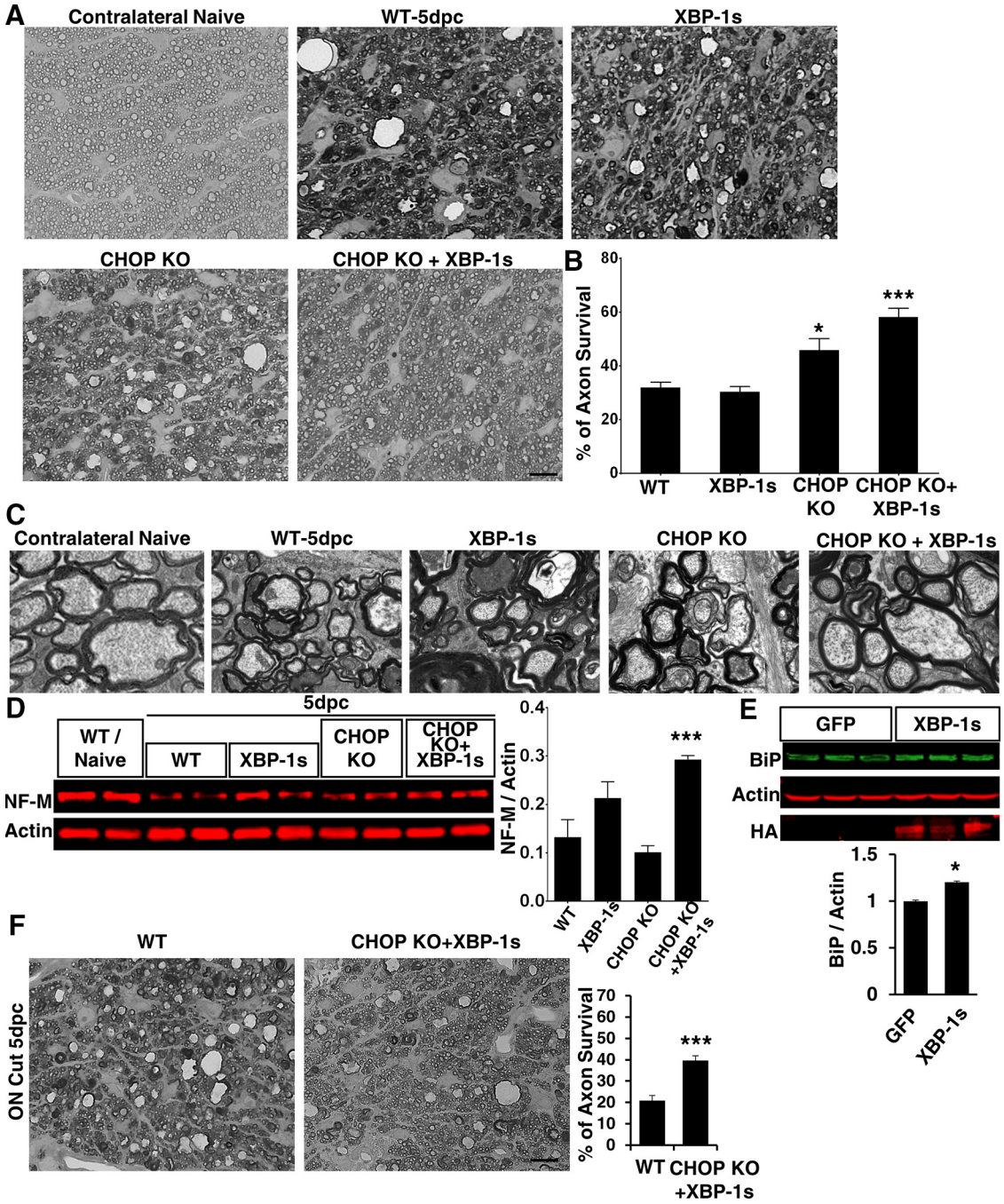

Figure 1. *CHOP* deletion and XBP-1 activation synergistically promote RGC axon survival at 5 dpc after ON injuries. ***A***, Representative light microscope images of semithin transverse sections of ON with PPD staining without crush (contralateral naive) or 5 dpc in WT and *CHOP* KO mice with or without XBP-1s overexpression. ***B***, Quantification of surviving axons in ON, represented as percentage of surviving axons in the injured ON, compared to the intact contralateral ON. $n = 7$. ***C***, Representative electron microscope images of transverse sections of ON (12,000× magnification). ***D***, Left, Western blot of ON lysates from biological duplicates/group showing expression levels of NF-M and actin. Right, Quantification of NF-M expression normalized to actin. $n = 6$. ***E***, Top, Western blot of retina lysates from three biological replicates showing expression levels of BiP, actin, and HA-tagged XBP-1s in WT mice with AAV-GFP or AAV-XBP-1s injection. Bottom, Quantification of BiP expression normalized to actin. $n = 3$. ***F***, Left, Representative light microscope images of semithin transverse sections of ON with PPD staining at 5 dpc after complete ON cut. Right, Quantification of surviving axons in ON, represented as percentage of surviving axons in the injured ON, compared to the intact contralateral ON. $n = 7$. Data are presented as means ± SEM. Scale bars: 10 μm. $^*p < 0.05$; $^{***}p < 0.001$ (***B***, ***D***, one-way ANOVA with Bonferroni's *post hoc* test; ***E***, ***F***, Student's *t* test).

ER stress manipulation preserves visual function in mouse glaucoma model

To determine the potential clinical importance of ER stress manipulation, we measured the VEP, a gross electrical signal recorded from the visual cortex after flash stimulation of the eye (Ridder and Nusinowitz, 2006). Because the VEP signal depends on the integrity of the entire visual pathway, including RGC somata and ON axons, it can serve as readout of the physiological function of both structures. We recorded the VEP from mice 1 week before microbead injection (baseline) and at 7 WPI (end point). Because the variation of P1–N1 amplitude was too large to be used in this model (data not shown), we focused on the more stable N1 and P1 latencies. N1 and P1 latencies were significantly prolonged in the glau-

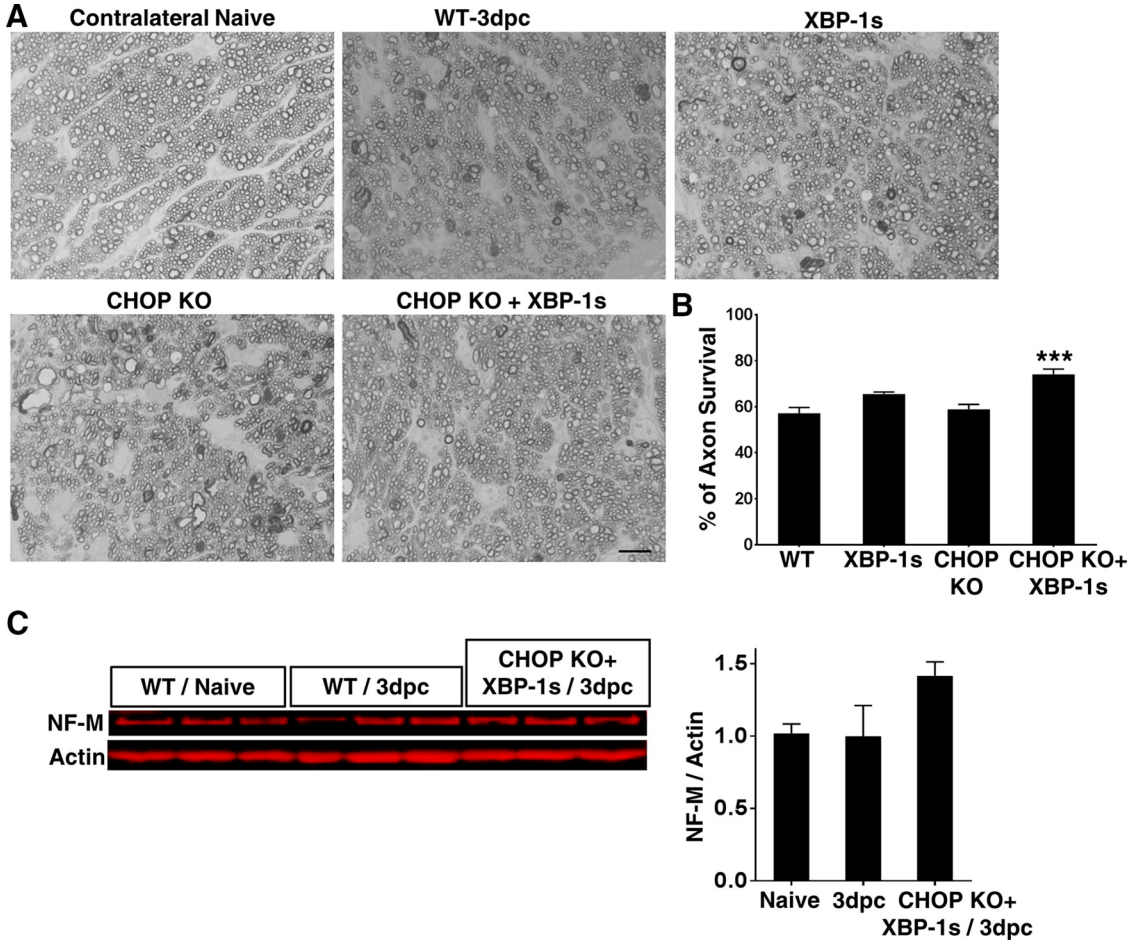

Figure 2. *CHOP* deletion and XBP-1 activation synergistically promote RGC axon survival at 3 dpc after ON crush. ***A***, Representative light microscope images of semithin transverse sections of ON with PPD staining without crush (contralateral naive) or 3 dpc. Scale bar, 10 μm. ***B***, Quantification of surviving axons in ON, represented as percentage of surviving axons in the injured ON, compared to the intact contralateral ON. $n = 7$. ***$p < 0.001$ (one-way ANOVA with Bonferroni's *post hoc* test). ***C***, Left, Western blot of ON lysates from three biological replicates per group showing expression levels of NF-M and actin. Right, Quantification of NF-M expression normalized to actin. $n = 3$. Data are presented as means ± SEM.

comatous eyes of WT mice; these changes were much smaller in mice with XBP-1 activation, *CHOP* deletion, or combined treatment, indicating preservation of visual function by ER stress manipulation (Fig. 4). It is worth noting that although XBP-1s alone did not significantly promote glaucomatous axon survival, it did improve VEP responses compared to controls, suggesting that the RGC somata protected by XBP-1s contributed directly to VEP signals.

Blocking eIF2α phosphorylation and activating XBP-1 promote neuroprotection of RGC somata and axons after ON crush

To confirm that the PERK-eIF2α-CHOP branch of UPR plays a detrimental role after axon injury, we conducted a similar analysis to test whether blocking the phosphorylation of eIF2α also provides neuroprotection. Since the homozygous eIF2α S51A mice are postnatal lethal (Scheuner et al., 2001), we used the *eIF2α A/A;fTg* transgenic mouse (Back et al., 2009), in which the homozygous eIF2α S51A mutant (which cannot be phosphorylated) replaces both alleles of endogenous WT eIF2α, and one copy of floxed WT eIF2α is ubiquitously expressed to overcome the postnatal lethality of homozygous eIF2α S51A. AAV-Cre injection in *eIF2α A/A;fTg* mice will delete the only copy of WT eIF2α, which is accompanied by expression of GFP as an indicator and effects the temporally controlled expression solely of the unphosphorylated eIF2α S51A mutant specifically in RGCs. We have confirmed that CHOP expression induced by ON crush was significantly decreased by removing the WT eIF2α and only expressing the eIF2α S51A mutant in RGCs (Fig. 5*A*). We also confirmed that the injection of the mixture of AAV-Cre and AAV-XBP-1s achieved high efficiency of WT eIF2α deletion and XBP-1s overexpression in RGCs (Fig. 5*B*), which resulted in both RGC soma and axon protection after ON crush. Blocking eIF2α-P alone, however, yielded better RGC soma protection and worse RGC axon protection than *CHOP* deletion. In addition, although eIF2α-P inhibition with XBP-1 activation achieved similar RGC soma protection, axon protection after ON crush was much worse than that provided by *CHOP* deletion with XBP-1 activation (compare Fig. 1*A*,*B*, Fig. 5*C*,*D*). These findings indicate that the neuroprotective effect of eIF2α-P inhibition was not exerted solely through CHOP inhibition. Similar to *CHOP* KO + XBP-1s mice, RGC soma protection was much better than axon protection in mice with eIF2α A/A + XBP-1s, which indicates that ER stress plays a more dominant role in neuron soma death than in axon degeneration.

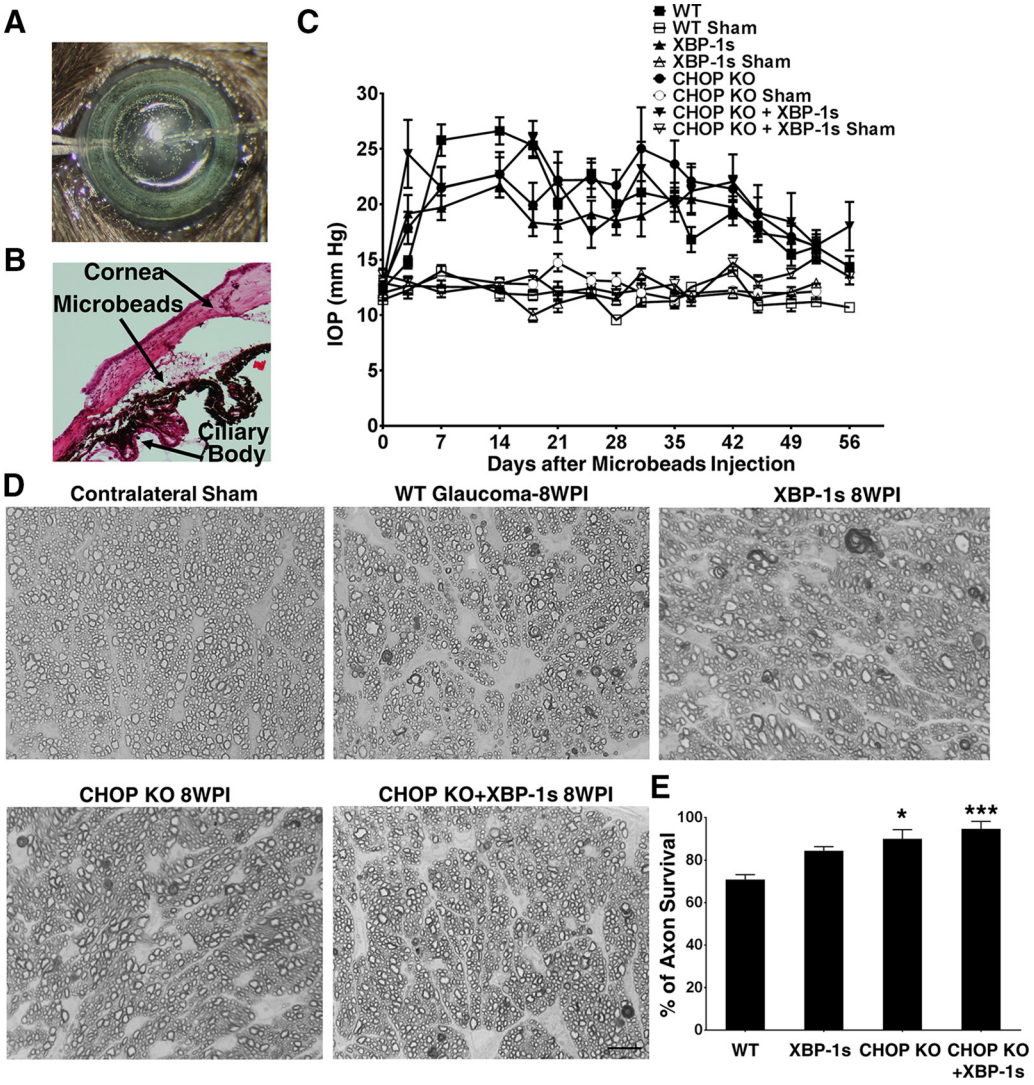

Figure 3. ER stress manipulation prevents glaucomatous RGC axon degeneration. ***A***, Injection of microbeads into the anterior chamber. ***B***, Paraffin section of mouse eye shows microbead accumulation. ***C***, IOP measurements of different treatment groups. ***D***, Representative light microscope images of semithin sections of ON with PPD staining at 8 WPI. Scale bar, 10 μm. ***E***, Quantification of surviving axons in ON. Data are presented as means ± SEM. WT, $n = 9$; AAV-XBP-1s, $n = 12$; *CHOP* KO, $n = 7$; *CHOP* KO + AAV-XBP-1s, $n = 11$. $^{*}p < 0.05$; $^{***}p < 0.001$ (one-way ANOVA with Bonferroni's *post hoc* test).

Blocking eIF2α phosphorylation and activating XBP-1 promote neuroprotection and preserve visual function in glaucoma model

Next we tested the combination of eIF2α-P inhibition and XBP-1s overexpression in the glaucoma model, which confirmed the neuroprotective effect of manipulating these two UPR pathways on glaucomatous RGC somata and axons (Fig. 6*A*,*B*). VEP analysis showed striking visual function protection as well, evidenced by significantly shorter P1 and N1 latencies in the eIF2α A/A glaucomatous eyes with or without AAV-XBP-1s injection than in WT mice (Fig. 6*C*,*D*). Similar to XBP-1s alone, the eIF2α A/A mutant did not significantly promote glaucomatous axon survival, but achieved better VEP, suggesting the importance of RGC soma protection for preserving visual function. Together, these results show that blocking CHOP upstream molecule eIF2α together with activating XBP-1 protects glaucomatous RGC somata and axons and, more importantly, preserves visual function.

Delayed ER stress manipulation also provides neuroprotection in glaucoma

To simulate the clinical setting, we tested whether manipulating UPR only after IOP elevation also protects RGC somata and axons. We used two strategies to manipulate UPR after IOP elevation: (1) AAV-mediated CHOP shRNA expression to knock down CHOP levels and (2) AAV-Cre-mediated blocking of eIF2α-P. We first confirmed that microRNA-based AAV-CHOP shRNA-GFP knocks down CHOP levels in cultured cells and retinas (Fig. 7*A*–*C*). We next injected AAV-CHOP shRNA + AAV-XBP-1s or AAV-scramble shRNA + AAV-GFP (control) in WT mice at 1 WPI, when IOP reaches its peak. Since AAV-mediated gene expression in RGCs normally peaks at least 2 weeks after infection (Hu et al., 2012; Boye et al., 2013), CHOP is likely to be inhibited and XBP-1s expressed in RGCs 2 weeks after IOP elevation. Importantly, this delayed ER stress modulation significantly protected RGC somata and axons (Fig. 7*D*,*E*). The treated eyes showed significantly less prolonged N1 latency and P1 latency than the

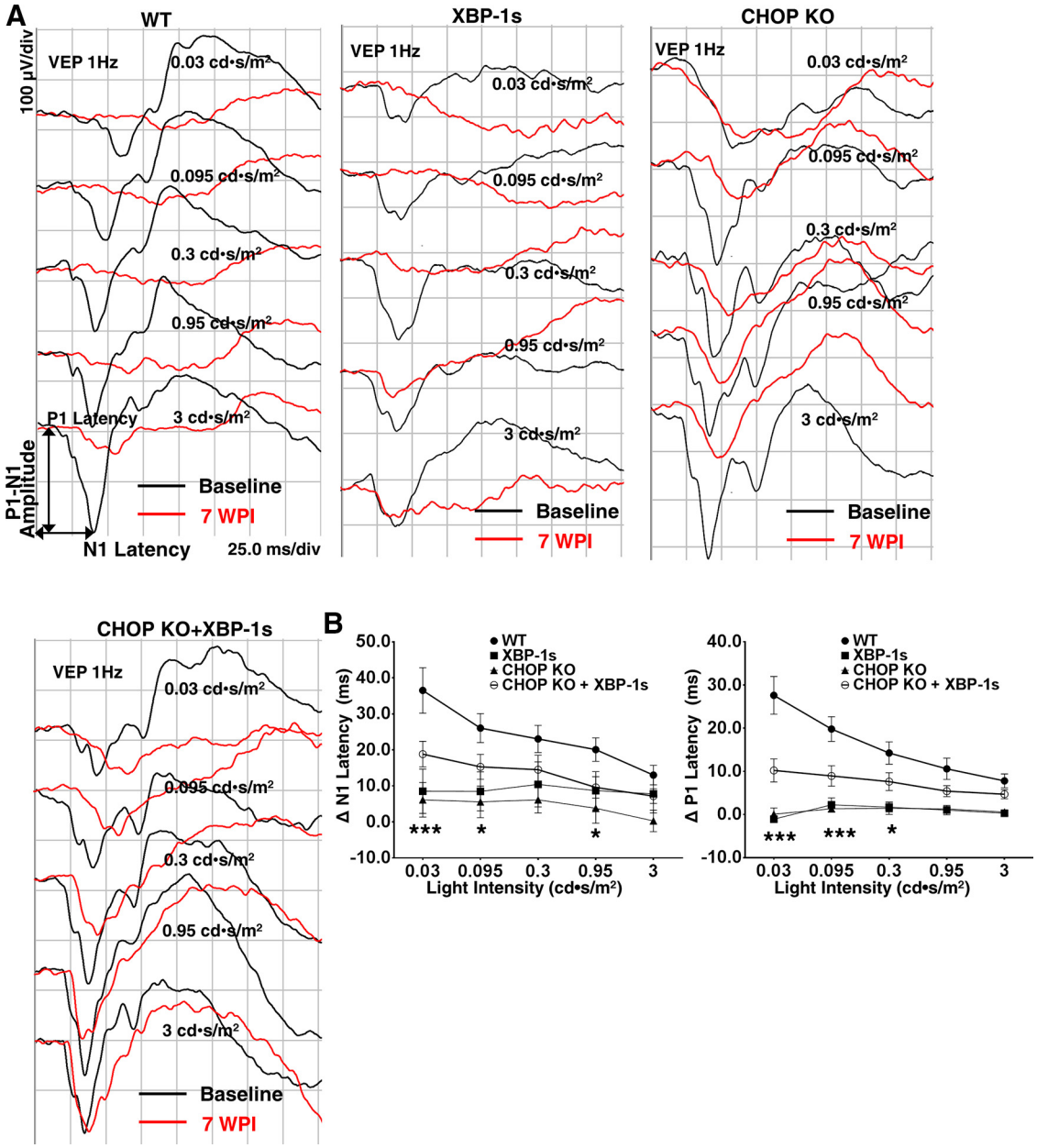

Figure 4. ER stress manipulation preserves visual function after IOP elevation. ***A***, Representative waveforms showing the VEP elicited by a series of stimulus light intensities. Black line, Baseline, 1 week before injection of microbeads. Red line, 7 WPI. ***B***, The differences in flash VEP responses between 1 week before and 7 weeks after microbead injection are represented as ΔN1 latency and ΔP1 latency in response to a series of varying stimulus light intensities. Data are presented as means ± SEM. WT, $n = 21$; AAV-XBP-1s, $n = 12$; *CHOP* KO, $n = 6$; *CHOP* KO + AAV-XBP-1s, $n = 19$. $^{*}p < 0.05$; $^{***}p < 0.001$ (two-way ANOVA with Bonferroni's *post hoc* test).

control eyes (Fig. 7*F*). Next we injected *eIF2α A/A;fTg* mice with AAV-Cre + AAV-XBP-1s at 1 WPI. Delayed inhibition of eIF2α-P and XBP-1 activation significantly protected RGC somata and axons and significantly spared visual function (Fig. 7*G–I*). Consistent with previous reports (Lin et al., 2007; Saxena et al., 2009; Hu et al., 2012; Moreno et al., 2012; Ma et al., 2013b), our results indicate that the PERK-eIF2α-CHOP branch of ER stress is toxic to injured neurons and that combined inhibition of this pathway and activation of the XBP-1 pathway is a promising therapeutic approach for glaucoma.

Discussion

Although neuroprotectants have long been sought, none has been found. Only deciphering the key upstream signals that trigger the degeneration cascade in both neuronal soma and axon will fulfill this significant unmet clinical need and lead to innovative and efficient neuroprotective treatments. By exploiting the anatomical and technical advantages of the RGC/ON system for studies of CNS traumatic injury (ON crush) and neurodegenerative diseases (glaucoma), we demonstrated that PERK-eIF2α-CHOP inhibition and XBP-1 activation preserves the structure and function of both RGC somata and axons. This result indicates the critical importance of ER stress in the pathophysiology of CNS axonopathies. Our findings that these two arms of UPR play opposite roles in neurodegeneration is consistent with the emerging theme that IRE1α-XBP-1activation occurs transiently in ER stress and is cell protective, whereas PERK-eIF2α-CHOP activation persists during chronic ER stress and triggers cell death (Rutkowski et al., 2006; Lin et al., 2007, 2009). CHOP has been

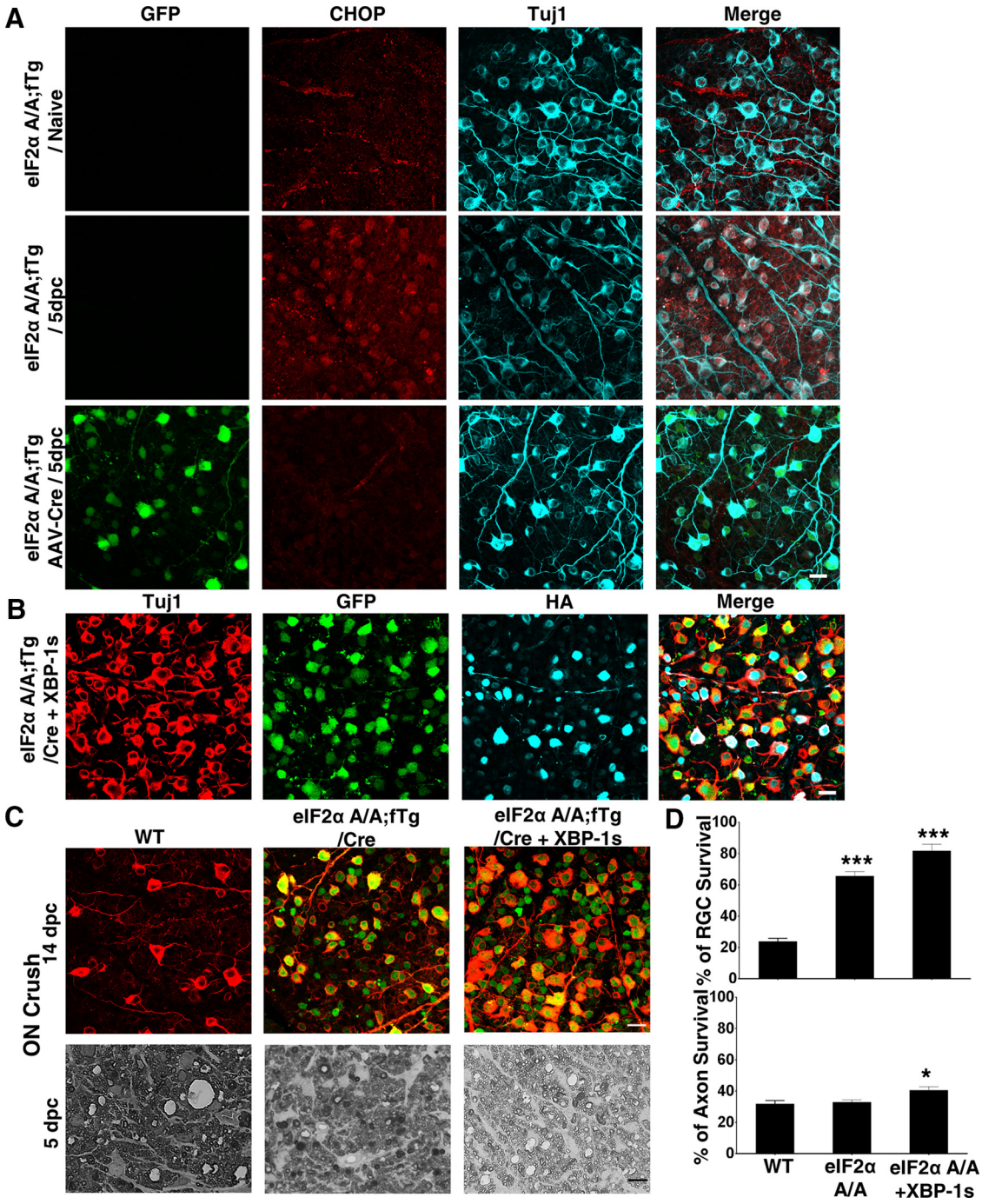

Figure 5. Blocking eIF2α phosphorylation and activating XBP-1 promote neuroprotection of RGC somata and axons after ON crush. ***A***, Representative confocal images of whole-mount retinas labeled with GFP, CHOP, Tuj1, and merged images. ***B***, Representative confocal images of whole-mount retinas 2 weeks after intravitreous injection of AAV-Cre + AAV-XBP-1s-HA in eIF2α A/A;fTg mice showing a majority of Tuj1 positive RGCs (red) are also GFP (Cre expression) and HA (XBP-1s-HA expression) positive. ***C***, Top, Whole-mount retinas showing surviving Tuj1 positive (red) and AAV-Cre positive (GFP) RGCs at 14 dpc. Bottom, Semithin sections of ON with PPD staining at 5 dpc. ***D***, Quantification of surviving RGCs at 14 dpc (WT, $n = 9$; eIF2α A/A, $n = 12$; eIF2α A/A + AAV-XBP-1s, $n = 8$) and surviving axons in ON at 5 dpc (WT, $n = 7$; eIF2α A/A, $n = 10$; eIF2αA/A + AAV-XBP-1s, $n = 9$). Scale bars: ***A***, ***B***, ***C***, top, 20 μm; ***C***, bottom, 10 μm. Data are presented as means ± SEM. *$p < 0.05$; ***$p < 0.001$ (one-way ANOVA with Bonferroni's *post hoc* test).

associated with apoptosis downstream of ER stress through down-regulating antiapoptotic Bcl2 (McCullough et al., 2001), upregulating proapoptotic BH-3-only molecules Bim (Puthalakath et al., 2007) and p53 upregulated modulator of apoptosis (Galehdar et al., 2010), increasing protein synthesis (Han et al., 2013), and stimulating death receptor 5 (Lu et al., 2014). Inhibition of CHOP is beneficial in multiple disease models (Zinszner et al., 1998; Oyadomari et al., 2002; Silva et al., 2005; Song et al., 2008; Hu et al., 2012). Moreover, *CHOP* KO is protective for injured motor neuron axons (Pennuto et al., 2008; Penas et al., 2011), and that an ER stress-protective agent attenuates axonal degeneration (Saxena et al., 2009). Thus, axon injury-induced neuronal ER stress could be a common mechanism for both neuronal soma and axon degeneration in a broad range of neurological diseases (Li et al., 2013). Although how ER stress is involved in axonopathies is unknown, UPR may play an intra-axonal role. Interestingly, XBP-1 splicing has been shown to

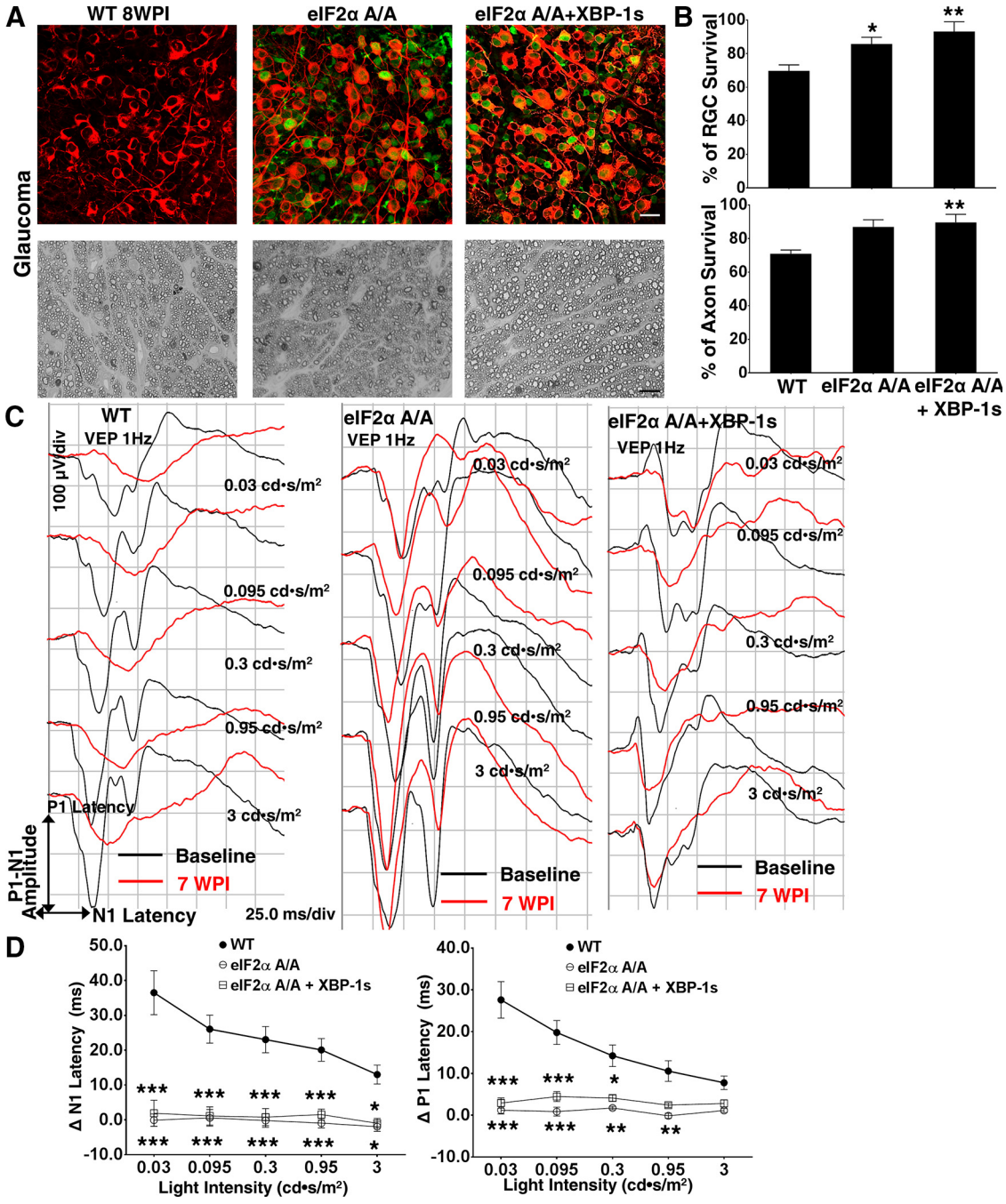

Figure 6. Blocking eIF2α phosphorylation and activating XBP-1 promotes neuroprotection and preserves visual function in glaucoma model. ***A***, Top, Whole-mount retinas showing surviving Tuj1 positive (red) and AAV-Cre positive (GFP) RGCs at 8 WPI (glaucoma model). Bottom, Semithin sections of ON with PPD staining at 8 WPI (glaucoma model). Scale bars: Top, 20 μm; bottom, 10 μm. ***B***, Quantification of surviving RGCs (WT, $n = 12$; eIF2α A/A, $n = 10$; eIF2αA/A + AAV-XBP-1s, $n = 10$) and surviving axons in ON at 8 WPI (WT, $n = 7$; eIF2α A/A, $n = 5$; eIF2αA/A + AAV-XBP-1s, $n = 9$). $^*p < 0.05$; $^{**}p < 0.01$ (one-way ANOVA with Bonferroni's *post hoc* test). ***C***, Representative waveforms showing the VEP elicited by a series of stimulus light intensities. Black line, Baseline, 1 week before injection of microbeads. Red line, 7 WPI. ***D***, The differences in flash VEP responses, represented as ΔN1 and ΔP1 latencies with a series of stimulus light intensities (WT, $n = 21$; eIF2α A/A, $n = 10$; eIF2α A/A + AAV-XBP-1s, $n = 11$). Data are presented as means ± SEM. $^*p < 0.05$; $^{**}p < 0.01$; $^{***}p < 0.001$ (two-way ANOVA with Bonferroni's *post hoc* test).

occur initially in neurites and to translocate to the nucleus later (Hayashi et al., 2007), and elevated levels of eIF2α-P and ATF4 have been detected in the axons of cultured neurons treated with Aβ1–42 (Baleriola et al., 2014). However, the interaction between RGC cell body and axon certainly makes an important contribution to the decision between death and survival, and the current injury models did not allow us to distinguish definitively the neuronal soma-autonomous from the axon-autonomous effects. The injury signals transported back to the neuronal soma from the injured axon may be critical; blocking them may protect both the neuronal soma and axon. We therefore propose that the UPR signaling molecules may have similar functions in response to axon injury as the previously identified dual leucine zipper kinase (DLK; Welsbie et al., 2013; Fernandes et al., 2014).

A paradox of the PERK- eIF2α-CHOP pathway is that although it can counteract ER stress and enable the cell to

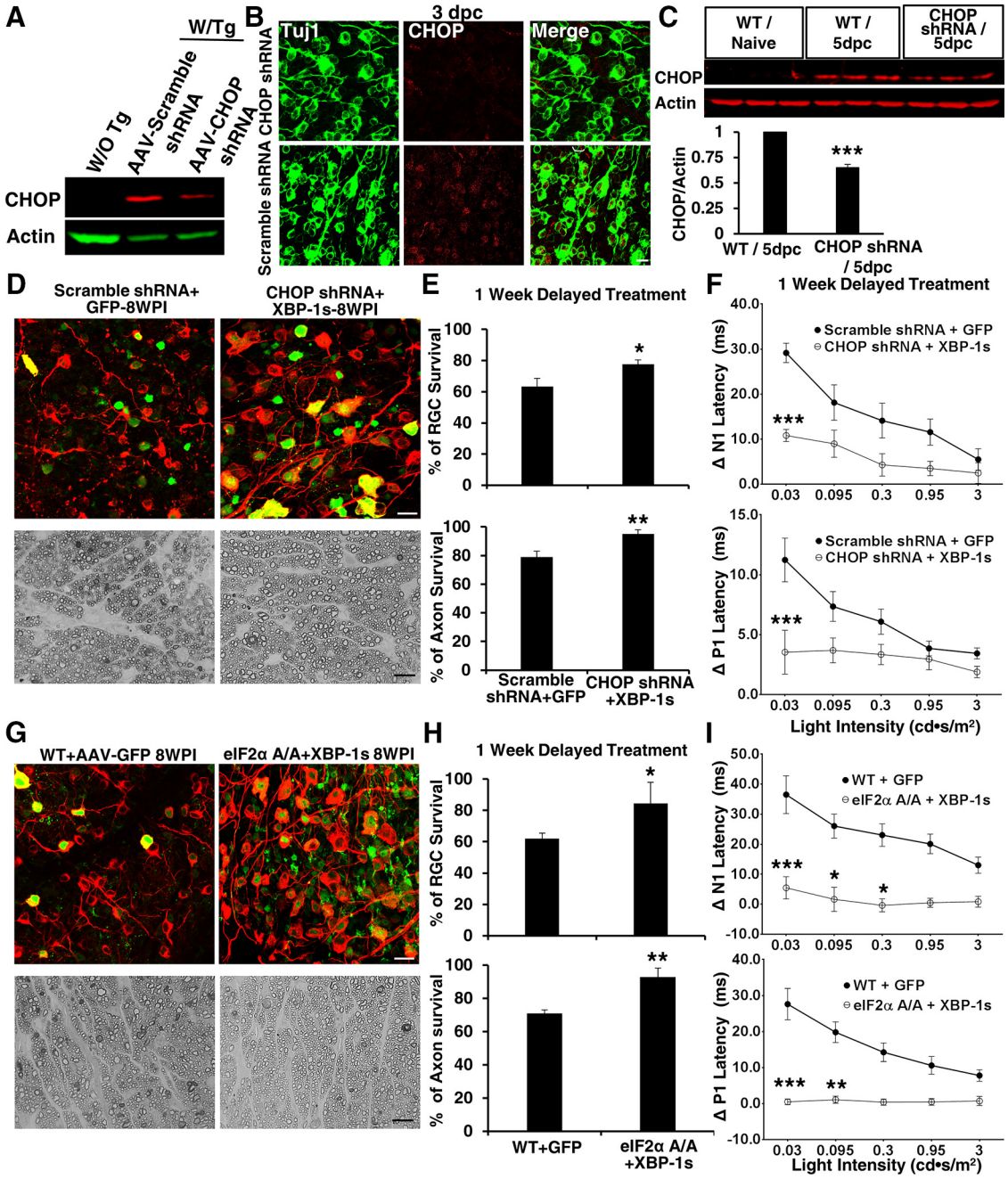

Figure 7. Delayed ER stress manipulation provides neuroprotection in glaucoma. ***A***, Western blot of CHOP expression in mouse 3T3 cells with AAV-Scramble shRNA-GFP or AAV-CHOP shRNA-GFP infection. Tg, Thapsigargin (ER stress inducer). ***B***, CHOP expression in whole-mount retinas at 3 dpc. Scale bar, 20 μm. ***C***, Top, Western blot of retina lysates from three biological replicates per group showing expression levels of CHOP and actin in WT naive mice or 5 dpc of WTs with or without AAV-CHOP shRNA injection. Bottom, Quantification of CHOP expression normalized to actin. $n = 3$. ***D***, ***G***, Top, Whole-mount retinas showing surviving Tuj1 positive (red) and GFP positive RGCs at 8 WPI. Bottom, Semithin sections of ON with PPD staining at 8 WPI. AAVs were injected intravitreally at 1 WPI. ***E***, ***H***, Top, Quantification of surviving RGCs. Bottom, Quantification of surviving axons in ON. ***F***, ***I***, The differences in the flash VEP responses are represented as ΔN1 latency and ΔP1 latency elicited by a series of stimulus light intensities. All quantification data are presented as means ± SEM (AAV-Scramble shRNA + AAV-GFP, $n = 6$; AAV-CHOP shRNA-GFP + AAV-XBP-1s, $n = 10$; eIF2α A/A;fTg mice with AAV-Cre + AAV-XBP-1s, $n = 6$; WT mice with AAV-GFP, $n = 21$). $^*p < 0.05$; $^{**}p < 0.01$; $^{***}p < 0.001$ (Student's *t* test was used for two-group comparisons and two-way ANOVA with Bonferroni's *post hoc* test was used for flash VEP data analysis). Scale bars: ***B***, ***D***, ***G***, top, 20 μm; ***D***, ***G***, bottom, 10 μm.

achieve a new homeostasis and survive, it also leads to cell death if ER stress is prolonged (Rutkowski et al., 2006). Phosphorylation of eIF2α inhibits cap-dependent mRNA translation and therefore attenuates ER stress by reducing the protein workload of ER. Thus, reduction of translation reduction by the PERK-eIF2α pathway enables pancreatic β cells and other cell types to adapt to ER stress and survive (Malhotra and Kaufman, 2007; Back et al., 2009). Similarly, sustained eIF2α-P by inhibition of eIF2α-P phosphatase promotes motor neuron survival in mouse models of chronic neurodegenerative diseases (Zhu et al., 2008; Saxena et al., 2009; Das et al., 2015). However, suppression of protein translation by eIF2α-P is not always protective, and emerging evidence indicates that blocking eIF2α-P is actually neuroprotective. Ele-

vated levels of eIF2α-P and axonally synthesized ATF4 have been detected in the brains of AD mice and patients and linked to neuronal cell death (Baleriola et al., 2014). Activation of the PERK/eIF2α branch may also be responsible for synaptic defects and neuronal degeneration in prion disease (Moreno et al., 2012, 2013) and AD (Ma et al., 2013b). In addition, downregulation of eIF2α-P by a PERK inhibitor or derepression of protein translation by small molecules results in potent neuroprotection (Axten et al., 2012; Ma et al., 2013b; Halliday et al., 2015). In the present study, we demonstrated that genetic blocking of eIF2α-P significantly increases RGC survival, indicating the similarity between optic neuropathies and other neurodegenerative diseases. The dissimilar neuroprotective effects of *CHOP* deletion and inhibition of eIF2α-P on RGC soma and axon signify that eIF2α-P plays a role in neurodegeneration that is CHOP independent. It will be of great interest to decipher the downstream mechanism by which eIF2α acts independently of blocking CHOP to contribute to neuroprotection. Because suppression of protein translation by eIF2α-P may block expression of cell survival proteins (Allagnat et al., 2011), resumption of protein synthesis after blocking eIF2α-P may enhance cell survival. Interestingly, eIF2α-P downregulates the translation of X-linked inhibitor of apoptosis (XIAP) in a CHOP-independent manner, which contributes to cell death induced by chronic ER stress (Hiramatsu et al., 2014). Future experiments will determine whether XIAP is upregulated in RGCs of eIF2α A/A mutant mice and, more intriguingly, whether *CHOP* deletion and eIF2α-P block act synergistically to promote neuroprotection.

In addition to Wld^{s} (Beirowski et al., 2008, 2009; Howell et al., 2013; Zhu et al., 2013; Conforti et al., 2014), several endogenous molecules have been found previously to promote axonal degeneration, including SARM (sterile α-motif-containing and armadillo-motif containing protein; Osterloh et al., 2012; Gerdts et al., 2013; Yang et al., 2015), PHR1 (an E3 ubiquitin ligase; Babetto et al., 2013), DLK (Welsbie et al., 2013), and the mitogen-activated protein kinase cascade (Miller et al., 2009; Yang et al., 2015). Inhibiting these molecules significantly enhances axon protection. It will be extremely interesting to investigate the potential cross talk between these pathways and the UPR pathways and to determine whether targeting them together has a synergistic neuroprotective effect.

The mechanism that induces ER stress in axonopathies is unknown. Influx of extracellular calcium and release of calcium from intra-axonal smooth ER are important early events after axon injury that correlate with initiation of axon degeneration (Wang et al., 2012; Howell et al., 2013), possibly by promoting cytoskeleton disintegration (Ma et al., 2013a) and mitochondrial dysfunction (Barrientos et al., 2011). Disturbance of calcium homeostasis is actually a major inducer of ER stress (Ron and Walter, 2007; Wang and Kaufman, 2012; Li et al., 2013). Thus, it is possible that intra-axonal calcium fluctuation early after axon injury induces ER stress, which then further increases intra-axonal calcium. Interestingly, calcium released from the ER can be taken up by mitochondria (Villegas et al., 2014), causing mitochondria dysfunction and axon degeneration (Barrientos et al., 2011; Court and Coleman, 2012; Villegas et al., 2014). Although this evidence places ER dysfunction upstream of mitochondria dysfunction, the reverse is also possible because redox changes and ATP depletion caused by mitochondria failure can induce ER stress. It is critical to determine which is the earlier event after axon injury, to establish the most promising clinical intervention target for neuroprotection.

Although axon degeneration is thought to be an active process of self-destruction that is mechanistically distinct from the process of apoptosis in the neuronal soma (Coleman and Perry, 2002; Raff et al., 2002; Whitmore et al., 2005; Saxena and Caroni, 2007; Wang et al., 2012), the two processes are sequentially connected. The protection of both neuronal soma and axon by ER stress manipulation indicates that axon injury-induced neuronal ER stress serves as a general upstream signal for both neuron apoptosis and axon autonomous degeneration. Optic neuropathies are likely to have mechanisms in common with other neurodegenerative diseases, such as ALS, AD, PD, and MS (Kersten et al., 2014). Our study therefore advances understanding of a mechanism essential for neuronal degeneration and provides information critical for the clinical application of ER stress modulation to preserve neural function in a wide range of acute and chronic neurodegenerative disorders.

References

Allagnat F, Cunha D, Moore F, Vanderwinden JM, Eizirik DL, Cardozo AK (2011) Mcl-1 downregulation by pro-inflammatory cytokines and palmitate is an early event contributing to beta-cell apoptosis. Cell Death Differ 18:328–337. CrossRef Medline

Axten JM, Medina JR, Feng Y, Shu A, Romeril SP, Grant SW, Li WH, Heerding DA, Minthorn E, Mencken T, Atkins C, Liu Q, Rabindran S, Kumar R, Hong X, Goetz A, Stanley T, Taylor JD, Sigethy SD, Tomberlin GH, et al. (2012) Discovery of 7-methyl-5-(1-{[3-(trifluoromethyl)phenyl]acetyl}-2,3-dihydro-1H-indol-5-yl)-7H-p yrrolo[2,3-d]pyrimidin-4-amine (GSK2606414), a potent and selective first-in-class inhibitor of protein kinase R (PKR)-like endoplasmic reticulum kinase (PERK). J Med Chem 55:7193–7207. CrossRef Medline

Babetto E, Beirowski B, Russler EV, Milbrandt J, DiAntonio A (2013) The Phr1 ubiquitin ligase promotes injury-induced axon self-destruction. Cell Reports 3:1422–1429. CrossRef Medline

Back SH, Scheuner D, Han J, Song B, Ribick M, Wang J, Gildersleeve RD, Pennathur S, Kaufman RJ (2009) Translation attenuation through eIF2alpha phosphorylation prevents oxidative stress and maintains the differentiated state in beta cells. Cell Metab 10:13–26. CrossRef Medline

Baleriola J, Walker CA, Jean YY, Crary JF, Troy CM, Nagy PL, Hengst U (2014) Axonally synthesized ATF4 transmits a neurodegenerative signal across brain regions. Cell 158:1159–1172. CrossRef Medline

Barrientos SA, Martinez NW, Yoo S, Jara JS, Zamorano S, Hetz C, Twiss JL, Alvarez J, Court FA (2011) Axonal degeneration is mediated by the mitochondrial permeability transition pore. J Neurosci 31:966–978. CrossRef Medline

Beirowski B, Babetto E, Coleman MP, Martin KR (2008) The WldS gene delays axonal but not somatic degeneration in a rat glaucoma model. Eur J Neurosci 28:1166–1179. CrossRef Medline

Beirowski B, Babetto E, Gilley J, Mazzola F, Conforti L, Janeckova L, Magni G, Ribchester RR, Coleman MP (2009) Non-nuclear Wld(S) determines its neuroprotective efficacy for axons and synapses *in vivo*. J Neurosci 29:653–668. CrossRef Medline

Boye SE, Boye SL, Lewin AS, Hauswirth WW (2013) A comprehensive review of retinal gene therapy. Mol Ther 21:509–519. CrossRef Medline

Calkins DJ, Horner PJ (2012) The cell and molecular biology of glaucoma: axonopathy and the brain. Invest Ophthalmol Vis Sci 53:2482–2484. CrossRef Medline

Chung KH, Hart CC, Al-Bassam S, Avery A, Taylor J, Patel PD, Vojtek AB, Turner DL (2006) Polycistronic RNA polymerase II expression vectors for RNA interference based on BIC/miR-155. Nucleic Acids Res 34:e53. CrossRef Medline

Coleman MP, Perry VH (2002) Axon pathology in neurological disease: a neglected therapeutic target. Trends Neurosci 25:532–537. CrossRef Medline

Conforti L, Gilley J, Coleman MP (2014) Wallerian degeneration: an emerging axon death pathway linking injury and disease. Nat Rev Neurosci 15:394–409. Medline

Court FA, Coleman MP (2012) Mitochondria as a central sensor for axonal degenerative stimuli. Trends Neurosci 35:364–372. CrossRef Medline

Das I, Krzyzosiak A, Schneider K, Wrabetz L, D'Antonio M, Barry N, Sigurdardottir A, Bertolotti A (2015) Preventing proteostasis diseases by

selective inhibition of a phosphatase regulatory subunit. Science 348:239–242. CrossRef Medline

Fernandes KA, Harder JM, John SW, Shrager P, Libby RT (2014) DLK-dependent signaling is important for somal but not axonal degeneration of retinal ganglion cells following axonal injury. Neurobiol Dis 69:108–116. CrossRef Medline

Galehdar Z, Swan P, Fuerth B, Callaghan SM, Park DS, Cregan SP (2010) Neuronal apoptosis induced by endoplasmic reticulum stress is regulated by ATF4-CHOP-mediated induction of the Bcl-2 homology 3-only member PUMA. J Neurosci 30:16938–16948. CrossRef Medline

Gerdts J, Summers DW, Sasaki Y, DiAntonio A, Milbrandt J (2013) Sarm1-mediated axon degeneration requires both SAM and TIR interactions. J Neurosci 33:13569–13580. CrossRef Medline

Halliday M, Radford H, Sekine Y, Moreno J, Verity N, le Quesne J, Ortori CA, Barrett DA, Fromont C, Fischer PM, Harding HP, Ron D, Mallucci GR (2015) Partial restoration of protein synthesis rates by the small molecule ISRIB prevents neurodegeneration without pancreatic toxicity. Cell Death Dis 6:e1672. CrossRef Medline

Han J, Back SH, Hur J, Lin YH, Gildersleeve R, Shan J, Yuan CL, Krokowski D, Wang S, Hatzoglou M, Kilberg MS, Sartor MA, Kaufman RJ (2013) ER-stress-induced transcriptional regulation increases protein synthesis leading to cell death. Nat Cell Biol 15:481–490. CrossRef Medline

Hayashi A, Kasahara T, Iwamoto K, Ishiwata M, Kametani M, Kakiuchi C, Furuichi T, Kato T (2007) The role of brain-derived neurotrophic factor (BDNF)-induced XBP1 splicing during brain development. J Biol Chem 282:34525–34534. CrossRef Medline

Hiramatsu N, Messah C, Han J, LaVail MM, Kaufman RJ, Lin JH (2014) Translational and posttranslational regulation of XIAP by eIF2alpha and ATF4 promotes ER stress-induced cell death during the unfolded protein response. Mol Biol Cell 25:1411–1420. CrossRef Medline

Howell GR, Soto I, Libby RT, John SW (2013) Intrinsic axonal degeneration pathways are critical for glaucomatous damage. Exp Neurol 246:54–61. CrossRef Medline

Hu Y, Park KK, Yang L, Wei X, Yang Q, Cho KS, Thielen P, Lee AH, Cartoni R, Glimcher LH, Chen DF, He Z (2012) Differential effects of unfolded protein response pathways on axon injury-induced death of retinal ganglion cells. Neuron 73:445–452. CrossRef Medline

Kersten HM, Roxburgh RH, Danesh-Meyer HV (2014) Ophthalmic manifestations of inherited neurodegenerative disorders. Nat Rev Neurol 10:349–362. CrossRef Medline

Li S, Yang L, Selzer ME, Hu Y (2013) Neuronal endoplasmic reticulum stress in axon injury and neurodegeneration. Ann Neurol 74:768–777. CrossRef Medline

Libby RT, Li Y, Savinova OV, Barter J, Smith RS, Nickells RW, John SW (2005) Susceptibility to neurodegeneration in a glaucoma is modified by Bax gene dosage. PLoS Genet 1:17–26. Medline

Lin JH, Li H, Yasumura D, Cohen HR, Zhang C, Panning B, Shokat KM, Lavail MM, Walter P (2007) IRE1 signaling affects cell fate during the unfolded protein response. Science 318:944–949. CrossRef Medline

Lin JH, Li H, Zhang Y, Ron D, Walter P (2009) Divergent effects of PERK and IRE1 signaling on cell viability. PLoS One 4:e4170. CrossRef Medline

Lu M, Lawrence DA, Marsters S, Acosta-Alvear D, Kimmig P, Mendez AS, Paton AW, Paton JC, Walter P, Ashkenazi A (2014) Opposing unfolded-protein-response signals converge on death receptor 5 to control apoptosis. Science 345:98–101. CrossRef Medline

Ma M, Ferguson TA, Schoch KM, Li J, Qian Y, Shofer FS, Saatman KE, Neumar RW (2013a) Calpains mediate axonal cytoskeleton disintegration during Wallerian degeneration. Neurobiol Dis 56:34–46. CrossRef Medline

Ma T, Trinh MA, Wexler AJ, Bourbon C, Gatti E, Pierre P, Cavener DR, Klann E (2013b) Suppression of eIF2alpha kinases alleviates Alzheimer's disease-related plasticity and memory deficits. Nat Neurosci 16:1299–1305. CrossRef Medline

Malhotra JD, Kaufman RJ (2007) Endoplasmic reticulum stress and oxidative stress: a vicious cycle or a double-edged sword? Antioxid Redox Signal 9:2277–2293. CrossRef Medline

McCullough KD, Martindale JL, Klotz LO, Aw TY, Holbrook NJ (2001) Gadd153 sensitizes cells to endoplasmic reticulum stress by down-regulating Bcl2 and perturbing the cellular redox state. Mol Cell Biol 21:1249–1259. CrossRef Medline

Miao L, Yang L, Huang H, Liang F, Ling C, Hu Y (2016) mTORC1 is necessary but mTORC2 and GSK3beta are inhibitory for AKT3-induced axon regeneration in the central nervous system. Elife 5:e14908. Medline

Miller BR, Press C, Daniels RW, Sasaki Y, Milbrandt J, DiAntonio A (2009) A dual leucine kinase-dependent axon self-destruction program promotes Wallerian degeneration. Nat Neurosci 12:387–389. CrossRef Medline

Moreno JA, Radford H, Peretti D, Steinert JR, Verity N, Martin MG, Halliday M, Morgan J, Dinsdale D, Ortori CA, Barrett DA, Tsaytler P, Bertolotti A, Willis AE, Bushell M, Mallucci GR (2012) Sustained translational repression by eIF2alpha-P mediates prion neurodegeneration. Nature 485:507–511. Medline

Moreno JA, Halliday M, Molloy C, Radford H, Verity N, Axten JM, Ortori CA, Willis AE, Fischer PM, Barrett DA, Mallucci GR (2013) Oral treatment targeting the unfolded protein response prevents neurodegeneration and clinical disease in prion-infected mice. Science Transl Med 5:206ra138. CrossRef

Osterloh JM, Yang J, Rooney TM, Fox AN, Adalbert R, Powell EH, Sheehan AE, Avery MA, Hackett R, Logan MA, MacDonald JM, Ziegenfuss JS, Milde S, Hou YJ, Nathan C, Ding A, Brown RH Jr, Conforti L, Coleman M, Tessier-Lavigne M, et al. (2012) dSarm/Sarm1 is required for activation of an injury-induced axon death pathway. Science 337:481–484. CrossRef Medline

Oyadomari S, Koizumi A, Takeda K, Gotoh T, Akira S, Araki E, Mori M (2002) Targeted disruption of the Chop gene delays endoplasmic reticulum stress-mediated diabetes. J Clin Invest 109:525–532. CrossRef Medline

Penas C, Verdú E, Asensio-Pinilla E, Guzmán-Lenis MS, Herrando-Grabulosa M, Navarro X, Casas C (2011) Valproate reduces CHOP levels and preserves oligodendrocytes and axons after spinal cord injury. Neuroscience 178:33–44. CrossRef Medline

Pennuto M, Tinelli E, Malaguti M, Del Carro U, D'Antonio M, Ron D, Quattrini A, Feltri ML, Wrabetz L (2008) Ablation of the UPR-mediator CHOP restores motor function and reduces demyelination in Charcot-Marie-Tooth 1B mice. Neuron 57:393–405. CrossRef Medline

Puthalakath H, O'Reilly LA, Gunn P, Lee L, Kelly PN, Huntington ND, Hughes PD, Michalak EM, McKimm-Breschkin J, Motoyama N, Gotoh T, Akira S, Bouillet P, Strasser A (2007) ER stress triggers apoptosis by activating BH3-only protein Bim. Cell 129:1337–1349. CrossRef Medline

Quigley HA, Broman AT (2006) The number of people with glaucoma worldwide in 2010 and 2020. Br J Ophthalmol 90:262–267. CrossRef Medline

Raff MC, Whitmore AV, Finn JT (2002) Axonal self-destruction and neurodegeneration. Science 296:868–871. CrossRef Medline

Ridder WH 3rd, Nusinowitz S (2006) The visual evoked potential in the mouse–origins and response characteristics. Vision Res 46:902–913. CrossRef Medline

Ron D, Walter P (2007) Signal integration in the endoplasmic reticulum unfolded protein response. Nat Rev Mol Cell Biol 8:519–529. CrossRef Medline

Rutkowski DT, Arnold SM, Miller CN, Wu J, Li J, Gunnison KM, Mori K, Sadighi Akha AA, Raden D, Kaufman RJ (2006) Adaptation to ER stress is mediated by differential stabilities of pro-survival and pro-apoptotic mRNAs and proteins. PLoS Biol 4:e374. CrossRef Medline

Saxena S, Caroni P (2007) Mechanisms of axon degeneration: from development to disease. Prog Neurobiol 83:174–191. CrossRef Medline

Saxena S, Cabuy E, Caroni P (2009) A role for motoneuron subtype-selective ER stress in disease manifestations of FALS mice. Nat Neurosci 12:627–636. CrossRef Medline

Scheuner D, Song B, McEwen E, Liu C, Laybutt R, Gillespie P, Saunders T, Bonner-Weir S, Kaufman RJ (2001) Translational control is required for the unfolded protein response and *in vivo* glucose homeostasis. Mol Cell 7:1165–1176. CrossRef Medline

Silva RM, Ries V, Oo TF, Yarygina O, Jackson-Lewis V, Ryu EJ, Lu PD, Marciniak SJ, Ron D, Przedborski S, Kholodilov N, Greene LA, Burke RE (2005) CHOP/GADD153 is a mediator of apoptotic death in substantia nigra dopamine neurons in an *in vivo* neurotoxin model of parkinsonism. J Neurochem 95:974–986. CrossRef Medline

Smith RS (2002) Systematic evaluation of the mouse eye: anatomy, pathology, and biomethods. Boca Raton, FL: CRC.

Song B, Scheuner D, Ron D, Pennathur S, Kaufman RJ (2008) Chop deletion reduces oxidative stress, improves beta cell function, and promotes cell survival in multiple mouse models of diabetes. J Clin Invest 118: 3378–3389. CrossRef Medline

Villegas R, Martinez NW, Lillo J, Pihan P, Hernandez D, Twiss JL, Court FA (2014) Calcium release from intra-axonal endoplasmic reticulum leads to axon degeneration through mitochondrial dysfunction. J Neurosci 34: 7179–7189. CrossRef Medline

Wang JT, Medress ZA, Barres BA (2012) Axon degeneration: molecular mechanisms of a self-destruction pathway. J Cell Biol 196:7–18. CrossRef Medline

Wang S, Kaufman RJ (2012) The impact of the unfolded protein response on human disease. J Cell Biol 197:857–867. CrossRef Medline

Welsbie DS, Yang Z, Ge Y, Mitchell KL, Zhou X, Martin SE, Berlinicke CA, Hackler L Jr, Fuller J, Fu J, Cao LH, Han B, Auld D, Xue T, Hirai S, Germain L, Simard-Bisson C, Blouin R, Nguyen JV, Davis CH, et al. (2013) Functional genomic screening identifies dual leucine zipper kinase as a key mediator of retinal ganglion cell death. Proc Natl Acad Sci U S A 110:4045–4050. CrossRef Medline

Whitmore AV, Libby RT, John SW (2005) Glaucoma: thinking in new ways-a role for autonomous axonal self-destruction and other compartmentalised processes? Prog Retin Eye Res 24:639–662. CrossRef Medline

Yang J, Wu Z, Renier N, Simon DJ, Uryu K, Park DS, Greer PA, Tournier C, Davis RJ, Tessier-Lavigne M (2015) Pathological axonal death through a MAPK cascade that triggers a local energy deficit. Cell 160:161–176. CrossRef Medline

Yang L, Miao L, Liang F, Huang H, Teng X, Li S, Nuriddinov J, Selzer ME, Hu Y (2014) The mTORC1 effectors S6K1 and 4E-BP play different roles in CNS axon regeneration. Nat Commun 5:5416. CrossRef Medline

Zhu Y, Fenik P, Zhan G, Sanfillipo-Cohn B, Naidoo N, Veasey SC (2008) Eif-2a protects brainstem motoneurons in a murine model of sleep apnea. J Neurosci 28:2168–2178. CrossRef Medline

Zhu Y, Zhang L, Sasaki Y, Milbrandt J, Gidday JM (2013) Protection of mouse retinal ganglion cell axons and soma from glaucomatous and ischemic injury by cytoplasmic overexpression of Nmnat1. Invest Ophthalmol Vis Sci 54:25–36. CrossRef Medline

Zinszner H, Kuroda M, Wang X, Batchvarova N, Lightfoot RT, Remotti H, Stevens JL, Ron D (1998) CHOP is implicated in programmed cell death in response to impaired function of the endoplasmic reticulum. Genes Dev 12:982–995. CrossRef Medline